SMITH, LENA M., M.S. Carbon Nanodot Uptake and their Effects on Macrophages Upon Challenge with Oxidized LDL and TNF-alpha. (2019)
Directed by Dr. Zhenquan Jia. 52 pp.

Atherosclerosis, a leading cause of cardiovascular disease worldwide, represents a global concern because of its large economic and public welfare burden. Macrophages play important physiological and pathological roles in the development of atherosclerosis. Carbon nanodots (CNDs), members of a new class of carbon-based nanoparticles, serve as novel candidates for biomedical applications including bioimaging, biosensing, drug delivery, and especially modulation of cardiovascular inflammation because of their fluorescence, stability, and antioxidant properties. However, the action of CNDs on the macrophages has not yet been explored. Tumor Necrosis Factor α (TNF-α) and oxidized low-density lipoprotein (oxLDL) are important mediators for the alteration of the expression of genes involved in inflammation-mediated atherosclerosis. OxLDL is internalized by macrophages, increasing secretion of proinflammatory cytokines and inducing foam cells formation as lipid accumulates. In this study, the effects of CNDs on TNF-α and oxLDL induced inflammation in macrophages were examined.

Our results demonstrate that CNDs have low toxicity and display dose- and time-dependent uptake within THP-1 human monocyte-derived macrophages; human monocytic cell lines were differentiated into macrophages by 12-*O*-tetradecanoylphorbol-13-acetate (TPA) treatment. Cotreatment with CNDs significantly reduced gene expression of the cytokine interleukin-8 (IL-8), monocyte chemoattractant protein-1 (MCP-1)/CCL2, and interleukin-1β (IL-1β) in the context of both TNF-α and oxLDL

mediated inflammation. Cotreatment with CNDs also reduced TNF-α mediated vascular cell adhesion protein 1 (VCAM-1) and intercellular adhesion molecule 1 (ICAM) gene expression, and oxLDL mediated TNF-α expression. This demonstrates the anti-inflammatory effects of CNDs. While internalization of oxLDL induces foam cell formation, CNDs ameliorated lipid uptake. Furthermore, CNDs reduced oxLDL induced cytotoxicity in THP-1 human monocyte-derived macrophages. Gene expression of Gamma-glutamate Cystine Ligase Catalytic Subunit (GCLc) and NADPH quinone dehydrogenase (NQO1), enzymes involved in reactive oxygen species (ROS) detoxification, was not altered by CNDs. However, NF-κB transcriptional activity, mediated by TNF-α and oxLDL, was decreased by CNDs treatment in macrophages. Collectively, this research provides evidence for the ability of CNDs to attenuate TNF-α and oxLDL induced inflammation in macrophages.

CARBON NANODOT UPTAKE AND THEIR EFFECTS ON MACROPHAGES UPON CHALLENGE WITH OXIDIZED LDL AND TNF-ALPHA

by

Lena M. Smith

A Thesis Submitted to
the Faculty of The Graduate School at
The University of North Carolina at Greensboro
in Partial Fulfillment
of the Requirements for the Degree
Master of Science

Greensboro
2019

Approved by

_____
Committee Chair

APPROVAL PAGE

This thesis written by Lena M. Smith has been approved by the following committee of the Faculty of The Graduate School at The University of North Carolina at Greensboro.

Committee Chair_____

Committee Members_____

_____

_____
Date of Acceptance by Committee

_____
Date of Final Oral Examination

TABLE OF CONTENTS

LIST OF TABLES

Page

LIST OF FIGURES

Page

CHAPTER I

INTRODUCTION

Cardiovascular Disease

Cardiovascular diseases (CVD) are a group of diseases of the heart and blood vessels, which include hypertension, stroke, myocardial infarction, peripheral vascular disease, and coronary artery disease [1]. CVD are the leading cause of death for both men and women both in the United States and worldwide [1, 2]. According to the World Health Organization, thirty-one percent of deaths worldwide, approximately 17.9 million per year, are attributed to cardiovascular diseases [3]. Cardiovascular diseases represent a global concern because of their large economic and public welfare burden. In the United States alone, CVD costs about $200 billion per year, including the cost of health care, medication, and lost productivity [2].

Because of demographic changes in the United States, including obesity and the aging population, CVD is projected to remain a health care concern in the future. In the United States alone, 70.2 percent of adults are obese or overweight, with the most dire projections predicting that this percentage will increase to 85 percent of the population by 2030 [4]. Because excess body weight is a well-known risk factor for cardiovascular disease, this increase in obesity will be accompanied by an increase in CVD [4]. The age structure of the US population is also projected to change, with the size of the population those age 65 and older doubling by 2050 [5]. As the population ages, the prevalence of

CVD also increases; 70 to 75 percent of 60 to 79-year-old people have one or more forms of CVD, compared to 40 percent of 40 to 59-years-old people [5]. Because of this increased prevalence, there is a crucial need to develop preventative and therapeutic treatments for CVD, including atherosclerosis.

Initiation of Atherosclerosis

Atherosclerosis is a precursor to many other cardiovascular diseases. In this chronic inflammatory disease, plaques composed of lipids, especially low- density lipoprotein (LDL), accumulate and are retained within the tunica intima of the arteries [6, 7]. These plaques decrease the diameter of the blood vessel and can partially or completely block blood flow, leading to heart attack and stroke [6].

Atherosclerosis starts with endothelial dysfunction, which is initiated by multiple factors, including increased modified LDL, free radicals, hypertension, smoking, and infection by viruses and bacteria [8]. However, no matter the initiating factors, atherosclerosis represents a chronic inflammatory process at each stage[8]. Injured endothelial cells (ECs) and existing macrophages secrete cytokines, such as tumor necrosis factor α (TNF-α), and chemokines, such as monocyte chemoattractant protein-1 (MCP-1)/CCL2, recruiting circulating monocytes to the site to the atherosclerotic lesion [7, 9]. Endothelial cells express vascular cell adhesion protein 1 (VCAM-1) and intercellular adhesion molecule 1 (ICAM), which initiate adhesion of monocytes [6]. Then monocytes migrate into tunica intima because of P and E selectin-dependent rolling [7]. These monocytes differentiate into macrophages, which engulf cellular debris and lipids [8, 9].

The Role of Macrophages in Atherosclerosis

Activated macrophages can generally be grouped into two categories- M1 and M2 macrophages. Classically activated or M1 macrophages are pro-inflammatory and differentiate in response to granulocyte macrophage colony-stimulating factor (GM-CSF) and interferon-γ signaling [6, 8, 10]. In response to inflammation, these macrophages upregulate expression of scavenger receptors and toll-like receptors (TLR), pattern-recognition receptors that regulate innate immunity[10]. Scavenger receptors mediate the internalization of bacterial endotoxins, cells fragments, and oxidized LDL (oxLDL); TLRs can also bind to oxLDL and cause macrophage activation in which cells produce and secrete proinflammatory factors, such as TNF-α, interleukin-1β (IL-1β), IL-12, and IL-23, and chemokines CXCL9, CXCL10, and CXCL11[6, 8, 10]. Activated macrophages also produce proteases and increased reactive oxygen species (ROS) and nitric oxide [10].

Alternatively activated or M2 macrophages are anti-inflammatory and can differentiate in response to macrophage colony stimulating factor (M-CSF) signaling [6, 8]. They are induced by Th2-type cytokines IL-4 and IL-13, secrete anti-inflammatory factors, such as IL-1 receptor agonist and IL-10, and are involved in tissue repair and remodeling [10]. The M1/M2 classification of macrophages has organizational value, but in complex inflammatory processes like atherosclerosis, overlapping patterns of activation often occur. Therefore, it may be more realistic to consider the M1/M2 classification as a continuum, instead of a dichotomy.

In progressing atherosclerotic plaques, there is often a complex and shifting balance between M1 and M2 macrophages. Macrophages can play an active role in inducing and magnifying inflammation, but they also can act beneficially to maintain a steady state or regression of the plaque by promoting the proliferation of smooth muscle cells (SMCs), and undergoing apoptosis and efferocytosis after oxLDL internalization [11]. Oxidized LDL is an important regulator and mediator of macrophage activity in atherosclerotic plaques [12]. OxLDL binds to scavenger receptors, the most important of which is cluster of differentiation 36 (CD36), and toll-like receptor 4 (TLR 4) [13, 14]. This internalization can lead to formation and accumulation of lipid peroxides and cholesterol esters as macrophages differentiate into foam cells [12]. In the first phase of atherosclerosis, this is protective because it minimizes the effect of LDL on ECs and SMCs. OxLDL attracts monocytes and stimulates expression of MCP-1, macrophage colony-stimulating factors, and endothelial adhesion molecules [8, 11]. Increased monocyte recruitment and macrophage proliferation exacerbate the inflammatory response as recruited cells secret proinflammatory molecules [8]. TNF-a, IL- 1, and M-CSF secretion stimulate transcription of the LDL receptor gene and increase oxLDL binding to ECs and SMCs [8]. In macrophages, oxLDL binding to TLR4 activates nuclear factor Kappa B (NF-κB), through the MyD88- dependent and TRAM-dependent pathways, leads to pro-inflammatory cytokine production in foam cells which exacerbates inflammation in a self-amplifying feedback loop [9, 15].

Continuous lipoprotein uptake and accumulation leads to the formation of more foam cells, which then store more lipids and increase the size of the plaque, forming fatty

streaks [16]. Macrophages and foam cells possess a decreased ability to migrate, so inflammation remains unresolved and increases because macrophages produce pro-inflammatory cytokines and chemokines and reactive oxygen species [6, 11]. Macrophages undergo apoptosis and necrosis and can form a necrotic core due to impaired clearance or efferocytosis of apoptotic cells, which furthers plaque formation [6, 11]. Maturing atherosclerotic lesions form a fibrous cap, the stability of which is influenced by macrophages which synthesize enzymes that catabolize collagen, a key component of the fibrous cap [9]. Proinflammatory cytokines increase the expression of collagenase by macrophages, increasing the chance of plaque disruption and thrombosis [9].

Reactive Oxygen Species and Atherosclerosis

One of the major factors in the initiation and progression of atherosclerosis is oxidative stress. Oxidative stress occurs when there is an imbalance in the production of reactive oxygen species (ROS) and the activity of antioxidant enzymes that regulate that ROS [17]. ROS are chemically active species containing oxygen, such as superoxide (O_2-•), hydrogen peroxide (H_2O_2), hydroxyl radical (OH•), and peroxynitrite (ONOO-)[17]. Increased ROS can be generated from from exogenous sources like pollutates and smoking or from inflammatory response which induces NADPH-oxidase, myeloperoxidase (MPO), and Inducible Nitric Oxide Synthase (iNOS) [15]. NADPH oxidase catalyzes the production of superoxide radical [18]. MPO catalyzes the formation of hypochlorous acid (HOCl) from hydrogen peroxide (H_2O_2), and chloride anion (Cl^-) [15]. iNOS is induced in response to inflammatory stimuli and produces nitric oxide

(NO) [18]. NO can react with superoxide to form peroxynitrite, which in moderate amounts increases the antibacterial activity of macrophages [18]. The production and release of ROS in macrophages, called oxidative burst, leads to the destruction of phagocytosed objects, such as invading pathogens, tumor cells, and endotoxins [18]. Therefore, ROS balance is critical of the immunological activity of macrophages.

While at low levels, ROS regulate cell function, at high-level ROS can lead to damage to cellular macromolecules, including oxidation of proteins, lipid peroxidation, and DNA damage. The activity of NADPH oxidase and myeloperoxidase can lead to the oxidation of LDL, which furthers foam cells formation and exacerbates inflammation [15]. Through the mitogen-activated protein kinases (MAPK) pathway, ROS can also activate NF-κB, increasing inflammation [15]. Through the nuclear factor erythroid 2–related factor 2 (Nrf2) pathway, ROS can also induce antioxidant responsive elements (ARE) in the promotor of antioxidant genes like glutathione peroxidase (GPX), superoxide dismutase (SOD), and glutathione reductase [15].

Current Treatments

Current treatments for CVD include medication such as statins, ACE inhibitors, and aspirin. These treatments can alter the progression of CVD by multiple mechanisms but are not without side effects. Statins inhibit 3-hydroxy-3-methylglutaryl coenzyme A (HMG-CoA) reductase, preventing the conversion of HMG-CoA to mevalonate [19]. This depletes intracellular cholesterol, which in turn up-regulates LDL receptor expression in the liver [19]. LDL clearance increases, and plasma cholesterol

concentration decreases [19]. Statins can also ameliorate oxidative stress; however, they have been linked to myalgia, peripheral neuropathy, and diabetes mellitus [19-22].

Angiotensin-converting-enzyme (ACE) inhibitors reduce hypertension by inhibiting ACE (kininase II), which cleaves Angiotensin I into Angiotensin II [23]. ACE inhibitors decrease carotid artery wall thickness and oxidative stress [23]. However, they can cause hypotension, hyperkalemia (increased blood-potassium), cough, and reversible decline in renal function [23]. Aspirin reduces the risk of myocardial infarction, but the effect on stroke and CVD is inconclusive [24]. While there are many therapeutic regimens available with the large public health impact of CVD, there is the demand for new treatments with few side effects.

Nanomedicine and Carbon Nanodots

There is currently interest in developing nanomaterials for biological application. The interdisciplinary research area of nanomedicine allows for the development of drug development systems with increased bioavailability and efficacy due to the targeting of drugs to specific tissues [25]. A wide variety of nanomaterials have been utilized for the targeted imaging of macrophages within cancer, atherosclerosis, and myocardial infarction [26]. For example, iron oxide particles conjugated with antibodies targeting oxidized phospholipids have been used in imaging of atherosclerotic lesions in mice [27]. However, since many nanoparticles are synthesized using heavy metals, there is concern about their safety in biomedical applications. Therefore, interest exists in the development of carbon-based nanoparticles, including graphene, nanotubes, fullerenes, and quantum dots. The development of quantum dots (QDs) represents an important

stage in the synthesis of carbon nanodots (CNDs). Quantum dots possess favorable qualities such as bright fluorescence, narrow emission range, high photostability, and resistance to degradation in biological systems [28]. However, QDs often contain toxic heavy metals like cadmium, which reduce their safety in biomedical applications [28]. Quantum dots can also produce ROS, causing oxidative stress and damaging cellular macromolecules [29]. CNDs are better candidates for biological applications because of their optical properties and low toxicity [28].

CNDs are quasi-spherical, carbon-based nanoparticles, with high oxygen content and a diameter of less than 10 nm [30]. CNDs are generated from two broad processes, either top-down or bottom-up assembly [30]. Top-down processes break down larger carbon-based molecules, such as carbon nanotubes, graphite columns or graphene, into smaller molecules using laser irradiation, electrochemistry, and chemical oxidation [28, 30]. Bottom-up processes utilize small organic precursors such as sucrose, amino acids, or food waste to build larger particles using microwaves, heat, or ultrasonic wave [28, 30].The goal of using different methods is to development synthesis methods, which are simple, cost-effective, and can be used at a large scale to generate size-controllable nanodots [28]. The processes described above synthesize unmodified CNDs, which can undergo surface modification and conjugation with other molecules [31].

CNDs possess many favorable characteristics, which are influenced by the surface modifications of the particle; these modifications can alter their fluorescent properties and interactions with a biological system [28]. Addition of highly hydrophilic surface groups increase water solubility and promote both wavelength-dependent and

independent photoluminescent (PL) in the visible range, which allows use for bioimaging and biosensing [30]. Conjugation of CNDs with specific receptors allows for high specificity for sensing intracellular molecules or targeting of specific cells for drug delivery [28, 30]. CNDs also display limited toxicity, which is influenced by surface modifications as well as the core particle [31-33]. This limited toxicity makes CNDs favorable candidates for multiple biological applications.

Multiple researchers have synthesized CNDs with the ability to scavenge free radicals. Zhang et al. preformed a microwave assisted synthesis of CNDs using citric acid and urea [34]. The ability of these CNDs to scavenge free radicals was accessed using 2,2-diphenyl-1-picrylhydrazyl radicals (DPPH·) [34]. In this assay, DPPH• is converted into a stable DPPH-H complex in the presence of an antioxidant, resulting in a purple to yellow color change that can be quantified by spectroscopy [35]. Zhang et al. observed a dose-dependent increase in scavenging of DPPH· radicals by their CNDs [34]. The same researchers also produced N,S-Codoped CNDs using a hydrothermal method with α-lipoic acid, citric acid, and urea precursors [32]. These CNDs also displayed increased DPPH· radical scavenging with increasing concentrations of nanoparticles [32]. While the two examples above display the *ex vivo* radical scavenging of CNDs, *in vitro* radical scavenging has also been observed. Das et al. synthesized CNDs by microwave irradiation of date molasses [33]. These displayed hydroxyl free radical inhibition in human MG 63 cells, a fibroblast cell line, according to Di-Chloro Di-Hydrofuran Fluorescein Di-Acetate (DCFH-DA) Assay [33]. They also observed *in vitro* superoxide inhibition as measured by NBT (Nitro Blue Tetrazolium) reduction assay [33]. The

results together suggest the antioxidant activity of CNDs *in vitro* and their potential application in scavenging free radicals.

Atherosclerosis is a chronic inflammatory disease in which plaque buildup narrows the walls of the arteries. Reactive Oxygen Species and subsequent oxidative stress play a crucial role in the initiation and progression of atherosclerosis by increasing inflammation and causing the oxidation of LDL. Macrophages are crucial mediators in inflammable vascular diseases, such as atherosclerosis. They can regulate inflammation by secreting pro-inflammatory cytokines and alter oxLDL metabolism. While CNDs are potential candidates for biomedical applications including biosensing, bioimaging, and drug delivery, the anti-inflammatory properties of CNDs on the macrophages within the cardiovascular system has not yet been explored. TNF-α and oxLDL are two essential mediators for the alteration of the expression of genes involved in inflammation. Currently, there is no report on CND impacts on macrophages, especially its anti-oxidative potential in mediating TNFα-induced and oxLDL induced macrophage injury. I hypothesized that the antioxidant properties of CNDs allow them to reduce TNFα-induced and oxLDL induced chemokine and adhesion molecule expression and subsequently protect against oxLDL toxicity on macrophages. We found that CNDs downregulate the expression of several inflammatory cytokines and chemokines induced by TNFα and oxLDL, in association with decreasing NFκB activation. CNDs also reduced oxLDL induced lipid accumulation and cytotoxicity within macrophages. By determining the impact of CNDs on macrophages, this study provides additional

information on their potential application in the treatment of atherosclerosis and other inflammatory diseases.

CHAPTER II

MATERIALS AND METHODS

Cell Culture

THP1 cells were cultured with RPMI-1640 media supplemented with 10% Fetal Bovine Serum (FBS) and 1 % Penicillin-Streptomycin. eLUCidate™ RAW 264.7, an NF-κB Reporter cell line, was cultured in Gibco® high glucose Dulbecco's Modified Eagle Medium (DMEM) with 10% FBS, 1% Penicillin-Streptomycin, and 3 μg/mL Puromycin. Media was renewed on alternating days. THP1 cells were induced to differentiate into macrophages by 12-O-tetradecanoylphorbol 13-acetate (TPA) treatment. 20 x 10^6 THP1 cells were cultured in Cellstar® Filter cap 175 cm^2 cell-culture treated filter screw cap flasks and treated with 1 ng/ml TPA in RMPI for three days (72 hours) in humidified incubators at 37 °C and 5% CO_2. Media was discarded on the third day, and new media was added. On the fourth day, cells were replated and various treatments were applied. Before treatment, cells were rinsed with 1X Phosphate Buffered Saline (PBS) and the supernant with cells was collected. The cells from the container surface were lifted by trypsin. Trypsin was neutralized by addition of RPMI completed with FBS and combined supernant with cells was centrifuged at 1,000 RPM for 7 minutes at 4 °C. The resulting harvested cells were suspended in Hank's Balance Salt Solution (HBSS), to avoid the influence of growth factor present in completed RPMI.Cells were

treated with carbon nanodots (CNDs) and/or Tumor Necrosis Factor α (TNFα) or oxidized Low-Density Lipoprotein (oxLDL) at various concentrations.

CND Synthesis

CNDs were synthesized by Wendi Zhang, a pHD student in Wei lab at the Joint School of Nanoscience and Nanoenginering (JSNN). 0.96g citric acid (CA), 1 ml Ethylenediamine (EDA), and 1 ml deionized water was mixed and heated in a microwave synthesizer (CEM Corp 908005) at 300W for 18 minutes. The resulting CNDs were dissolved in DI water and dialyzed through a dialysis membrane with MWCO (molecular weight cut-out) of 1000Da for 24 hours.

CND Characterization

The Cary® Eclipse TM Fluorescence Spectrophotometer was used to carry out UV-Vis spectroscopy of CNDs. CNDs were diluted to 0.06 mg/ml in DI-H_2O and measured for fluorescence in a quartz cuvette to determine their emission and excitation wavelengths.

Nexin™

4 x10^6 THP-1 human monocyte-derived macrophages per dish were treated with 0.01, 0.03, 0.1, and 0.3 mg/ml CNDs for 24 hours in Hank's Balance Salt Solution (HBSS) media in 100 mm × 10 mm Corning® cell culture-treated Petri dishes. After treatment, cells were rinsed with 1x PBS and lifted via cell scraper. Cells were counted, and diluted in 1x Annexin Binding Buffer to 1x10^6 cells/ml. 100 µl of cell suspension was transferred to a 1.5 mL Eppendorf® tube and stained with 2.5 µl FITC Annexin V and 1µl Propidium Iodide (PI). Cells were gently mixed and incubated for 15 minutes at

room temperature. After adding 400 µl 1X Binding Buffer to the stained cells, samples were analyzed by the Guava® easyCyte Flow Cytometry System and the percentage of viable, apoptotic, and dead cells were determined.

CND Uptake

4 x10^6 THP-1 human monocyte-derived macrophages per dishes were treated with CNDs at concentrations of 0, 0.01, 0.03, 0.1, and 0.3 mg/mL for incubation times of 3, 6, 12, and 24 hours in 100 mm × 10 mm Corning® cell culture-treated Petri dishes in HBSS. After treatment, cells were rinsed with 1x PBS and lifted via cell scraper. Cells were centrifuged at 5000 rpm for 5 minutes at 4 °C, and the resulting pellet suspended in 900 µl PBS. 300 µL of suspended cells were transferred in triplicate to a black opaque 96 well plate. Fluorescence was read at 360/460 top 400nm in a Synergy 2.0 well plate reader.

Oxidation of LDL

Five mg/ml Human Low-Density Lipoprotein (LDL) in 0.05M TRIS-HCl buffer, with 0.15M NaCl and 0.3mM EDTA, and pH 7.4 was purchased from Alfa Aesar. The LDL was dialyzed at 4 ˚C in 1x PBS for 24 hours to remove macromolecules greater than 2,000 Daltons and buffer salts. The resulting volume of LDL was measured and diluted with an equal volume 20 µM $CuSO_4$ in a light-sensitive tube. LDL was incubated at 37˚C for 12 hours to complete oxidation. OxLDL was used immediately for treatment and diluted in HBSS for final concentrations of 25 to 500 µg/mL.

Quantitative Real-Time Polymerase Chain Reaction (qRT- PCR)

For all qRT-PCR, 4 x10^6 THP-1 human monocyte-derived macrophages per dish were treated in 100 mm × 10 mm Corning® cell culture-treated Petri dishes in HBSS. Cell were treated with carbon nanodots (CNDs) and/or Tumor Necrosis Factor α (TNFα) or oxidized Low-Density Lipoprotein (oxLDL) at various concentrations.

For one treatment, cells were treated with 5 ng/µl TNFα for 3, 6, 12, and 24 hours. Macrophages were also treated with 1, 2, 5, and 10 ng/µl TNFα for 24 hours. For all TNF-α cotreatments, macrophages were treated with 10 ng/ µl TNFα and 0.01, 0.1, and 0.3 mg/ml CNDs for 24 hours. For oxLDL treatment, macrophages were treated with 25, 50, and 100 µg/ml oxLDL for 6 hours. For all oxLDL cotreatments, macrophages were treated with 100 µg/ml oxLDL and 0.01, 0.1, and 0.3 mg/ml CNDs for 6 hours. For CNDs alone treatments, cells were treated with 0.01, 0.03, 0.1, and 0.3 mg/ml CNDs for 24 hours.

After cells are treated as described above, the media was collected and centrifuged to collect any detached cells. Cells were transferred to an RNAase-free hood. RNA was isolated from cells, both the detached cells and cells attached to the Petri dishes, using TRizol™ Reagent according to ThermoFisher Scientific™ RNA isolation protocol. Isolated RNA was diluted in 15 µl RNase-free diethylpyrocarbonate (DEPC)-treated water.

Purity and concentration of the resulting RNA were determined by Thermo Scientific™ Nanodrop 2000, a full-spectrum UV-Vis spectrophotometer and normalized to 500 ng/µl. cDNA was synthesized by reverse transcription in Applied Biosystems™

Veriti™ 96 Well Thermal Cycler. This required using 5 µL 5x First Strand Buffer, 1.25 µL Random Primers, 1.25 µL deoxynucleotide triphosphate (dNTP) solution, 0.625 µL Moloney Murine Leukemia Virus Reverse Transcriptase (M-MLV RT), 14.875 µL DEPC-treated water, and 2 µL RNA per sample.

Resulting cDNA of genes of interest was amplified using Applied Biosystems™ StepOnePlus™ Real-Time PCR System for 40 cycles at the following settings: 95 °C for 15 seconds, 58 °C for 1 minute, and 60 °C for 15 seconds. Targets genes were Il-8, ICAM, VCAM, IL-1β, CCL2, TNF-α, GCLc, NQO1, and CD206 with GAPDH serving as the housekeeping gene. For each gene, primer master mix was made with 10 µL Power SYBR® Green PCR Master Mix, 5 µL DEPC-treated water, and 2 µL each of 5 µM forward and reverse primers, and 1 µl diluted cDNA (1:9). Threshold **(**C_T**)** values were compared to quantify gene expression.

Table 1. Primer Sequence for PCR Reactions

Target Gene	Forward primer	Reverse primer
GAPDH	5'- CGACCACTTTGTCAAGCT CA – 3'	5'- AGGGGTCTACATGGCAAC TG – 3'
IL-8	5'- CTCTGTGTGAAGGTGCAG TT – 3'	5'- AAACTTCTCCACAACCCTC TG – 3'
ICAM	5'- GGCTGGAGCTGTTTGAGA AC – 3'	5'- ACTGTGGGGTTCAACCTC TG - 3'
VCAM	5'-TGTCTGCTCAGATTGGAG AC–3'	5'-TCTGGATCTCTAGGGAATGA GTAG-3'
CCL2	5'-CCCAGTCACCTGCTGTT AT–3'	5'-TGGAATCCTGAACCCACT TC–3'
TNF-α	5'- CTATCTGGGAGGGGTCTT CC – 3'	5'- GGTTGAGGGTGTCTGAAG GA – 3'
IL-1β	5'- CAGCCAATCTTCATTGCT CA – 3'	5'- TCGGAGATTCGTAGCTGG AT – 3'
CD206	5'- CCTACTGGACACCAGGC AAT – 3'	5'- CAACCCAGTCCGTTTTT GAT – 3'
GCLc	5'-ACCATCATCAATGGGAAG GA – 3'	5'- GCGATAAACTCCCTCATC CA – 3'
NQO1	5'–TTACTATGGGATGGGGTC CA – 3'	5' –TCTCCCATTTTTCAGGCA AC – 3'

Oil Red O Staining

THP-1 human monocyte-derived macrophages were cotreated with 100 μg/mL oxLDL and 0.01 to 0.3 mg/mL CNDs for 6 hours. Cells were treated in Lab-Tek® 2 well chamber slides, with 4.2 x 10^5 cells per chamber. Oil Red O (ORO) staining was performed as described by Dr. Alan Daughtery [36]. Briefly, saturated stock ORO solution was diluted and filtered before use. Treated cells were fixed with 4% paraformaldehyde. Before staining, slides were washed with 60% isopropyl alcohol. Slides were stained for 10 minutes with filtered ORO, then washed with 60% isopropyl

alcohol and distilled water. Slides were then stained for 10 seconds with Hematoxylin and rinsed with distilled water. Cover slips were mounted onto the slide using glycerol gelatin. Slides were viewed, and images were taken using a Keyence BZ-X710 fluorescence microscope. To quantify the percentage of cells stained with ORO, images were viewed and counted using Image J software. Cells whose area were 30% or more stained dark red were counted as stained.

NF-κB RAW 264 Renilla Luciferase Assay

eLUCidate™ RAW 264.7, a NF-κB Reporter cell line was grown to a density of 1 X 10^5 cells per well in 6 well plates and treated with 30 ng/mL TNF-α or 100 μg/mL oxLDL with and without 0.3 mg/mL CNDs. After incubation, HBSS was decanted, and cells were washed with PBS twice. 1 mM coelenterazine was dissolved in PBS to a concentration of 1 μL coelenterazine per 1 mL PBS. 500 μL of this solution was added to each well. The luminescence intensity was measured directly after by Biotech Synergy 2 plate reader and normalized to untreated cells.

MTT Assay

THP-1 human monocyte-derived macrophages were cultured in clear 24-well Costar® cell-culture treated plates at a density of 8 x 10^4 cells/well in HBSS. For one treatment, cells were treated with 0, 50, 100, 200, 300, 400, and 500 μg/mL oxLDL for 6 hours. For another treatment, cells were cotreated with 400 μg/mL oxLDL and 0.1 or 0.3 mg/mL CNDs for 6 hours. After incubation for 6 hours, 0.2 mg/mL of 3-(4,5-dimethythiazol- 2-yl)-2,5-diphenyl tetrazolium bromide (MTT) diluted in PBS (3 mg MTT/ 1.5 mL PBS) was added to each well. Treated cells were incubated for 3.5 hours in

a humidified incubator at 37 °C and 5% CO_2. After incubation, the media and cells were collected in microcentrifuge tubes and washed with PBS. Macrophages were centrifuged at 5000 rpm for 5 minutes. Media was decanted, and cells were washed in 500 µL PBS. After cells were centrifuged again at 5000 rpm for 5 minutes and the supernatant removed, 600 µL of MTT reagent containing 50% DEPC water, 40% Isopropanol, and 10% dimethyl sulfoxide (DSMO), was added to each microcentrifuge tube. The cell pellet was dissolved with in the reagent, and the mixture was transferred in triplicate to a 96 well plate so for each condition, there were three wells of 200 µL mixture per well. Then, the plate was shaken at low speed for 5 minutes, allowing the formazan crystals to dissolve. To determine cell viability, absorbance at 570 nm was measured using the Bio-Tek® Synergy 2™ plate reader and normalized to untreated cells.

CHAPTER III

RESULTS

THP1 Differentiation

THP-1 cells were treated with 0-10 ng/μL 12-O-tetradecanoylphorbol-13-acetate (TPA) for 72 hours in RPMI media to induce differentiation into macrophages. The gene expression level of Cluster of Differentiation 206 (CD206), a macrophage differentiation marker whose expression is significantly increased in macrophages compared to monocytes, was assessed via qRT- PCR. As shown in Figure 1, increased gene expression ($P < 0.05$) of CD206 was observed in TPA treated cells for 72 hours, compared to untreated cells.

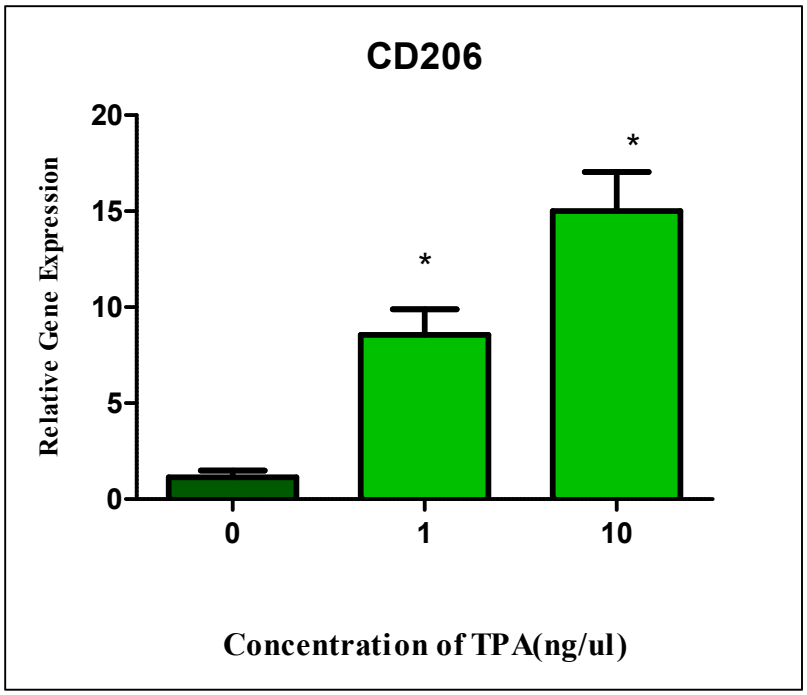

Figure 1. Increase in CD206 Expression in TPA Treated Cells. THP1 cells were treated with 0, 1, and 10 ng/ml of 12-O-tetradecanoylphorbol 13-acetate (TPA) in RPMI media for 72 hours. RNA was isolated, converted to cDNA, and assayed for CD206 using SYBR green qRT-PCR reagents via QuantStudio 3. GAPDH was the housekeeping gene. All data represent mean ± SEM. ($n = 3$, $P < 0.05$ vs. control)

Cell Viability Determined by Annexin-FITC Flow Cytometry

To determine the effect of CNDs on cell viability in THP-1 human monocyte-derived macrophages, I performed Annexin-FITC flow cytometry. Annexin-FITC flow cytometry measures stages of necrotic or apoptotic cell death through the binding of FITC Annexin V and Propidium Iodide (PI) dyes. Cells were treated with 0-0.3 mg/mL CNDs for 24 hours. FITC-Annexin V/7- AAD flow cytometry demonstrated CNDs at concentrations of 0.01 to 0.3 mg/ml, do not significantly change ($P< 0.05$) cell viability compared to untreated cells (Fig. 2a). Representative flow cytometric analysis (Figure 2b) show that the percentage of unstained cells in the lower left quadrant, do not differ significantly between CND treated and untreated cells ($P < 0.05$).

A

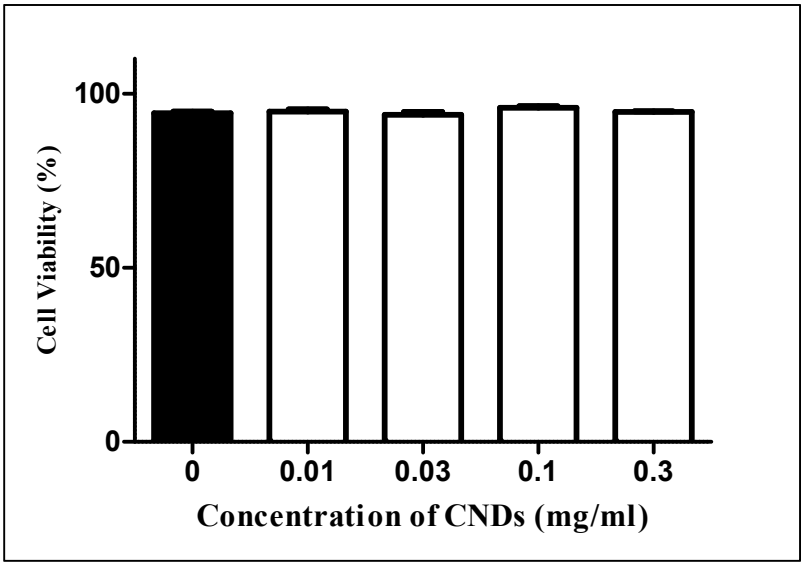

B

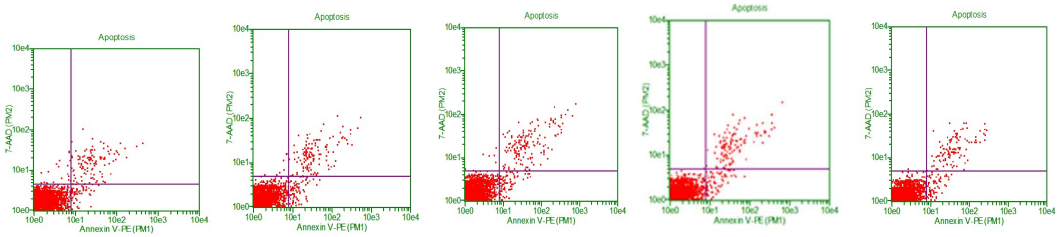

0 mg/ml 0.01 mg/ml 0.03 mg/ml 0.1 mg/ml 0.3 mg/ml

Figure 2. Effect of CNDs on Cell Viability. THP-1 human monocyte-derived macrophages were treated with various concentrations of CNDs in HBSS for 24 hours. (a) Cells were stained with 7-AAD and Annexin/PI to determine cell viability using flow cytometry analysis via Guava EasyCyte. (b) Representative flow cytometric analysis. From left to right: control, 0.01 mg/ml CNDs, 0.03 mg/ml, 0.1 mg/ml CNDs, 0.3 mg/ml CNDs. All data represent mean ± SEM (n=3). One-way ANOVA showed no significant differences in cell viability.

Characterization of CNDs and CND Uptake in THP1 Human-Derived Macrophages

To verify the photoluminescence of the nanoparticles used in this study, ultra-violet spectrophotometry was conducted on CNDs at a concentration of 0.06 mg/mL; this concentration was chosen to moderate the intensity of the excitation and emission, generating a distinguished peak but a gradual slope. The fluorescence spectrophotometry shows that CNDs exhibit fluorescence spectra consisting of a maximum excitation wavelength of 348 nm and a maximum emission wavelength of 461 nm (Fig. 3a).

Using this intrinsic fluorescence, I examined the intracellular uptake of CNDs in THP-1 human monocyte-derived macrophages. THP-1 human monocyte-derived macrophages were treated with CNDs at concentrations of 0, 0.01, 0.03, 0.1, and 0.3 mg/mL for incubation times of 3, 6, 12, and 24 hours. Cells were harvested, resuspended in PBS, and the fluorescence was read at 360/460 top 400nm in a Synergy 2.0 well plate reader. To quantify the weights of CNDs entering cells, a carbon nanodot standard was created by measuring the fluorescence of known concentrations of CNDs (Fig. 3b). A line of regression was generated and used to determine CND uptake. THP-1 human monocyte-derived macrophages showed a significant ($P<0.05$) dose-dependent increase in CND internalization at all time points (Fig. 4). The internalization was also time-dependent with a greater weight of CNDs (ng) per 1 million cells at 24 hours (Fig. 4d), compared to 12 hours (Fig. 4c). These results suggest that the intracellular uptake of CNDs occurs in a dose-dependent and time-dependent manner.

A

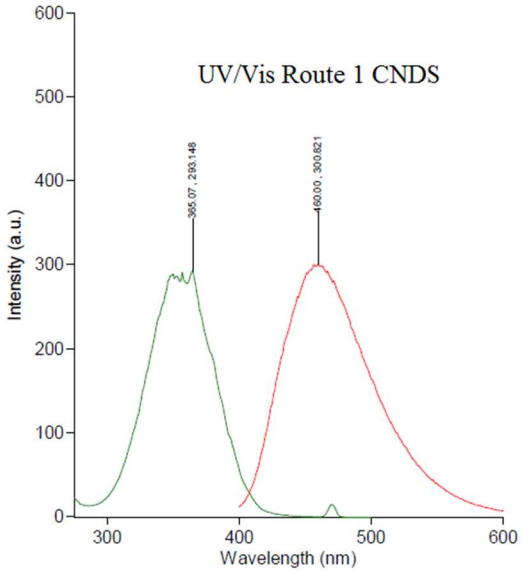

Figure 3. Characterization of CNDs. (a) The Excitation and emission of carbon nanodots were characterized using Cary fluorescence spectrophotometer. Excitation peak is at 365.07 nm, and the emission peak is at 460 nm. (b) CND standard curve. To quantify the weight of CNDs entering cells, a carbon nanodot standard was created by measuring the fluorescence of known concentrations of CNDs via microplate reader, and a line of regression was created.

B

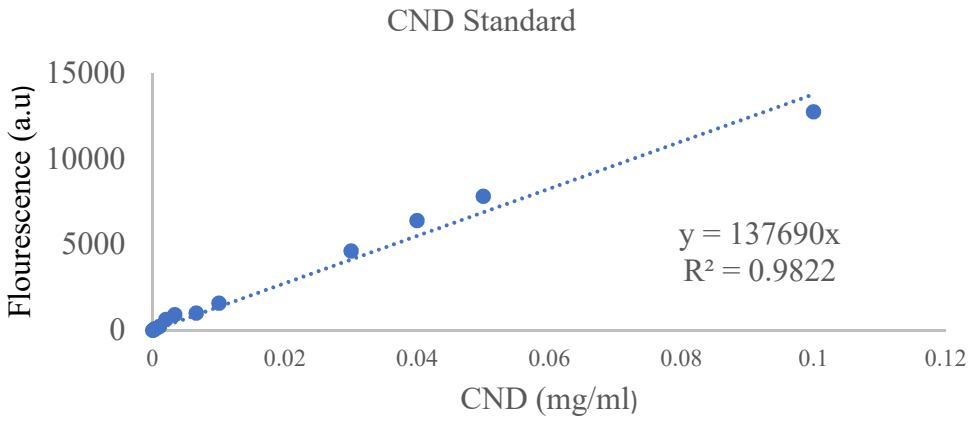

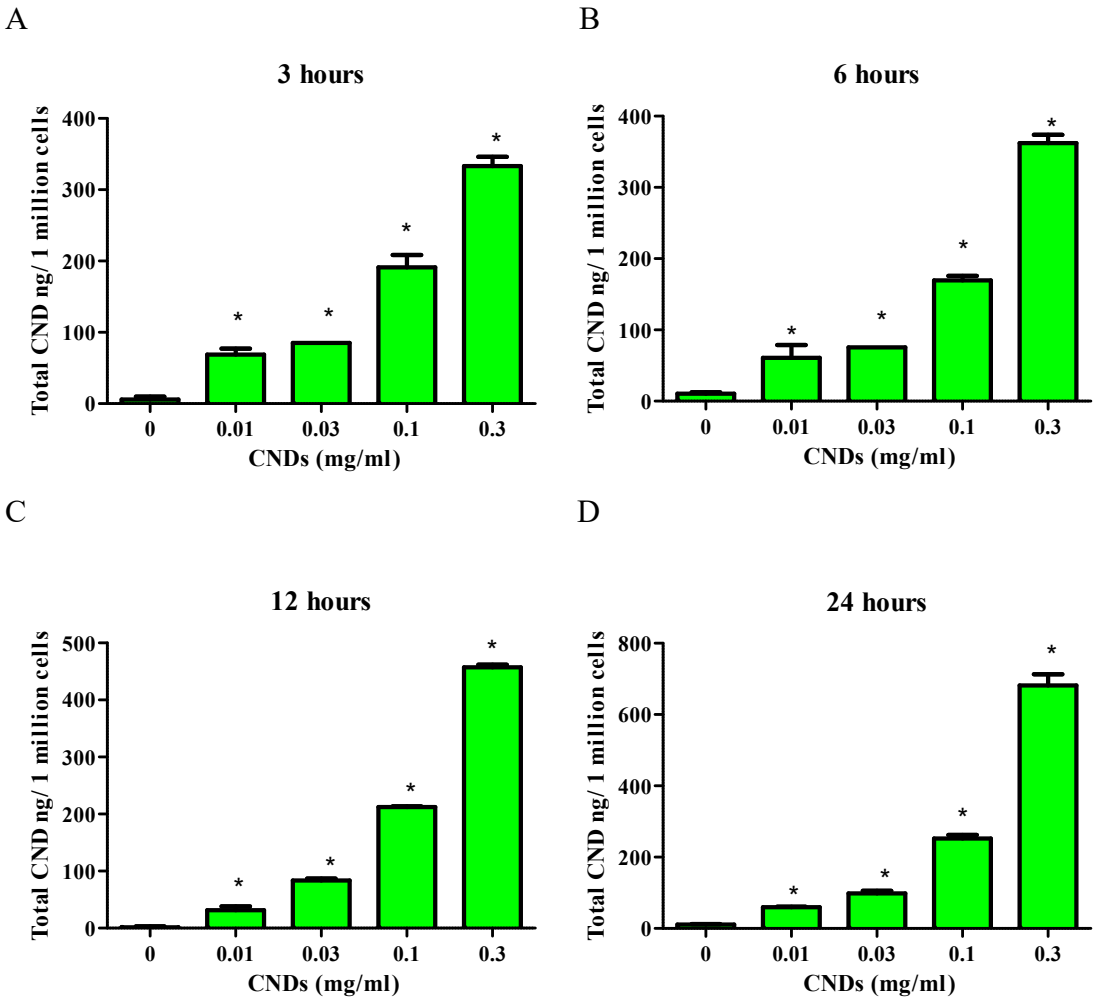

Figure 4. CND Uptake by THP-1 Human Monocyte-Derived Macrophages. Cells treated with 0.01-0.3 mg/mL CNDs in HBSS, collected and respuspened in PBS. Fluorescence was quantified using Bio-Tek Synergy 2.0 microplate reader. Using a standard curve, nanodot uptake was calculated. (a) Cells treated with 0.01-0.3 mg/mL CNDs for (a) 3 hours, (b) 6 hours, (c) 12 hours, and (d) 24 hours showed a dose dependent increase in total CNDs (ng) per 1 million cells. *All data represent mean ± SEM. ($n = 3$, $P < 0.05$ vs. control)*

CNDs Decrease the Expression of Pro-inflammatory Genes Induced by TNFα

Atherosclerosis is mediated by various pro-inflammatory genes. Since TNF-α is a known mediator of inflammation, I first investigated the concentration-dependent effect of TNF-α, on the inflammation markers in THP-1 human monocyte-derived macrophages. These cells were treated with1, 2, 5, and 10 ng/ml TNF-α diluted in HBSS for 24 hours. Using qRT-PCR, the relative gene expression of IL-8, VCAM, and ICAM were analyzed. As shown in Figure 5, TNF-α significantly increased ($P< 0.05$) expression of the target genes at multiple tested concentrations, with the greatest increases for IL-8 and VCAM being observed with 10 ng/ml treatment. As such, 10 ng/ml of TNF-α was the chosen concentration for co-treatments with CNDs. THP-1 human monocyte-derived macrophages were then treated with 0.01, 0.1 and 0.3 mg/ml CNDs and 10 ng/ml TNF-α in 5 mL HBSS for 24 hours. CND co-treatment at all concentrations significantly decreased ($P< 0.05$) TNF-α induced expression of IL 8 (Fig. 6A), and ICAM (Fig. 6C) compared to cells treated with TNF-α alone. As shown in Figure 6B, mRNA expression of VCAM significantly decreased ($P< 0.05$) when cotreated with 0.01 and 0.3 mg/mL CNDs ($P< 0.05$). Expression of IL-1β (Fig. 6D) and CCL2 (Fig 6E) significantly decreased ($P< 0.05$) in cells cotreated with the two highest concentrations of CNDS compared to cells treated with TNF-α alone.

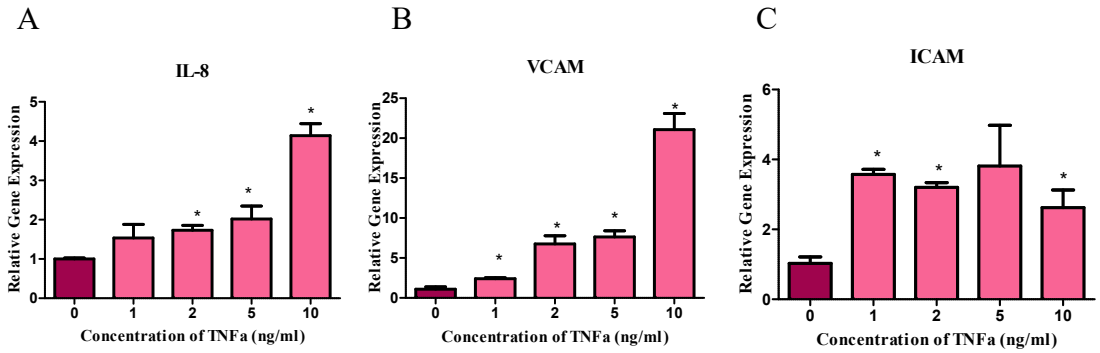

Figure 5. Dose-dependent Response due to TNF-α. THP-1 human monocyte-derived macrophages were treated 0-10 ng/mL TNF-α for 24 hours in HBSS. RNA was isolated, converted to cDNA, and assayed for IL-8, VCAM, and ICAM using SYBR green qRT-PCR reagents via QuantStudio 3. (a) Shows a significant increase in IL-8 expression when treated with 2, 5, and 10 ng/ml TNF-α. (b) Shows a significant increase in VCAM expression when treated with 1, 2, 5, and 10 ng/ml TNF-α. (c) Shows a significant increase in ICAM expression when treated with 1, 2, and 10 ng/ml TNF-α. GAPDH was the housekeeping gene. *All data represent mean ± SEM. ($n = 3$, $P < 0.05$ vs. control)*

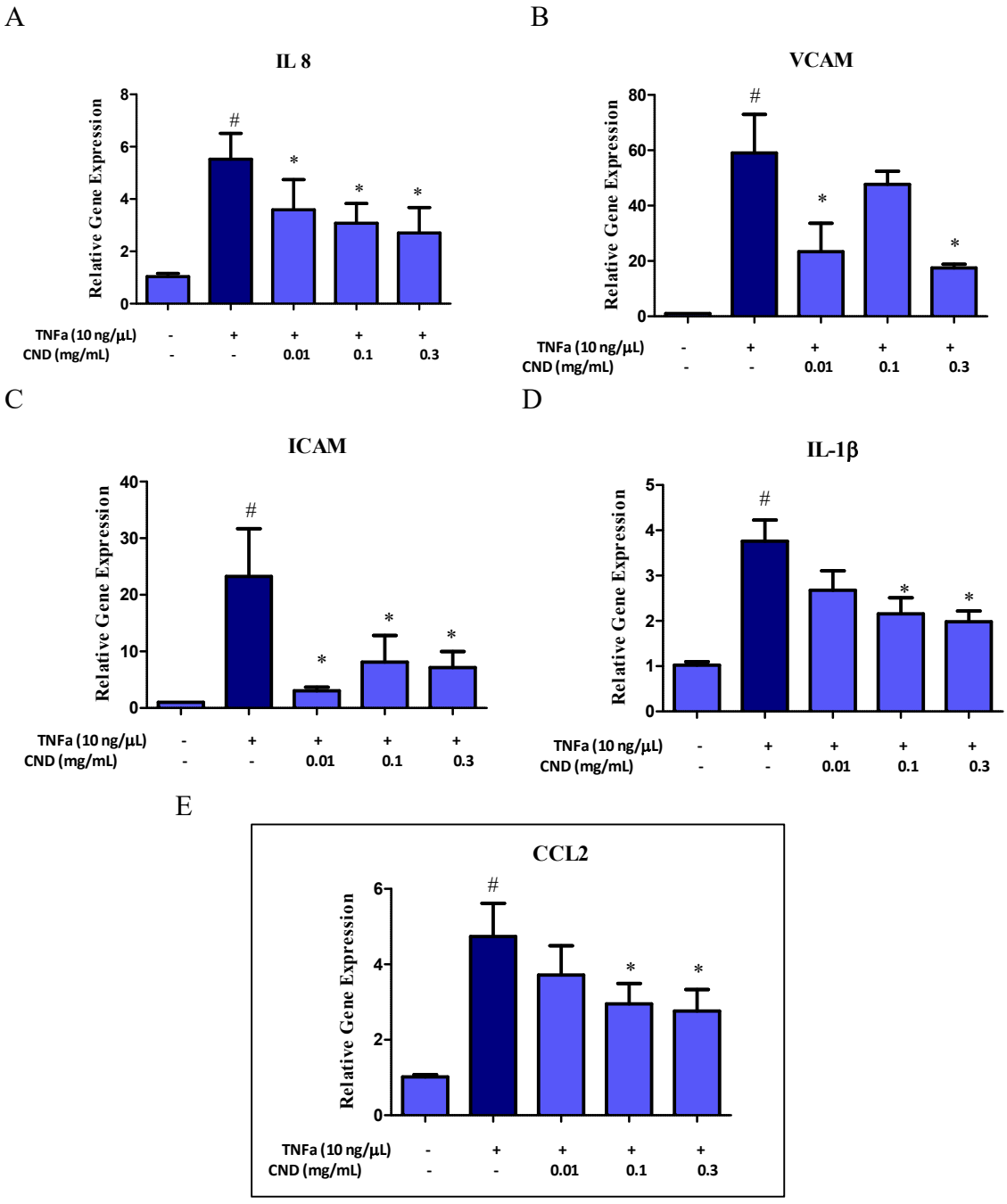

Figure 6. CNDs Decrease the Expression of Pro-Inflammatory Genes Induced by TNFα in THP-1 Human Monocyte-Derived Macrophages. THP-1 human monocyte-derived macrophages were cotreated with 0.01-0.3 mg/mL CNDs and 10 ng/mL TNF-α for 24 hours in HBSS. RNA was isolated, converted to cDNA, and assayed for IL-8, VCAM, ICAM, IL -1β, CCL2, and TNF-α using SYBR green qRT-PCR reagents via QuantStudio 3. (a) Shows a significant decrease in IL 8 expression when cotreated with

10 ng/mL TNF-α and 0.01 and 0.3 mg/mL for CNDs 24 hours. (b) Shows a significant decrease in VCAM expression when cotreated with 10 ng/mL TNF-α and 0.01-0.3 mg/mL for CNDs 24 hours. (c) Shows a significant decrease in ICAM expression when cotreated with 10 ng/mL TNF-α and 0.01-0.3 mg/mL for CNDs 24 hours. (d) Shows a significant decrease in IL -1β expression when cotreated with 10 ng/mL TNF-α and 0.1 and 0.3 mg/mL for CNDs 24 hours. (e) Shows a significant decrease in CCL2 expression when cotreated with 10 ng/mL TNF-α and 0.1 and 0.3 mg/mL for CNDs 24 hours. GAPDH was the housekeeping gene. All data represent mean ± SEM. (n = 9, #, $P < 0.05$ vs. control, * $P < 0.05$ vs. TNF-α)

Effect of CNDs on the Expression of ROS Detoxification Genes GCLC and NQO1

Reactive oxygen species can induce inflammation by causing oxidative stress. Cellular antioxidant glutathione (GSH) and ROS detoxification enzyme NADPH quinone dehydrogenase (NQO1) can reduce oxidative stress resulting in inflammation by neutralizing ROS. Therefore, to determine the impact of CNDs on the gene expression levels of Gamma-glutamate Cystine Ligase Catalytic Subunit (GLCc), an enzyme involved in GSH synthesis, and NQO1, THP-1 human monocyte-derived macrophages were treated with 0-0.3 mg/mL CNDs for 24 hours in HBSS. Using qRT-PCR, the relative gene expression of GLCc and NQO1 was determined. There was no significant change ($P< 0.05$) in GLCc expression (Fig 7A) or NQO1 expression (Fig 7B) in CND treated cells compared to untreated cells.

A

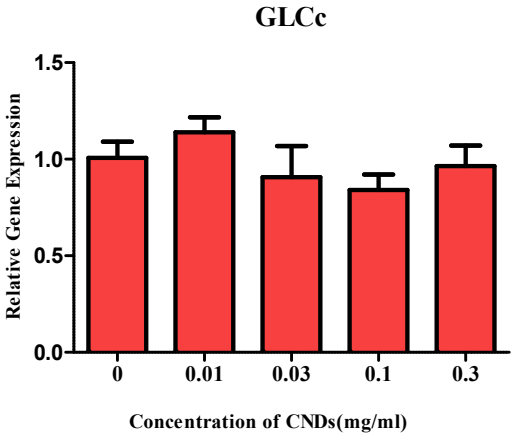

B

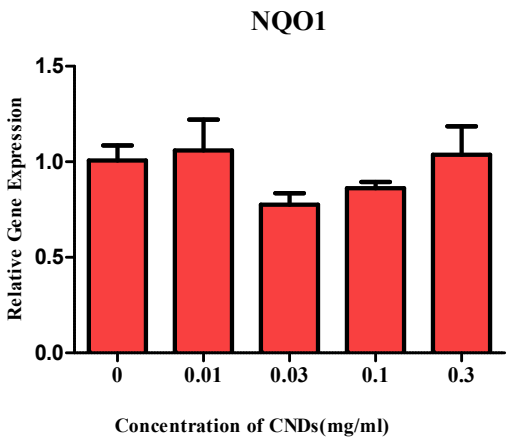

Figure 7. Effect of CNDs on Gene Expression of ROS Detoxification Genes GCLc and NQO1. THP-1 human monocyte-derived macrophages were treated with 0.01-0.3 mg/mL CNDs of 24 hours in HBSS. RNA was isolated, converted to cDNA, and assayed for GLCc and NQO1 using SYBR green qRT-PCR reagents via QuantStudio 3. (a) There was no significant change in GLCc expression. (b) There was no significant change in NQO1 expression. *All data represent mean ± SEM. ($n = 3$, $P < 0.05$ vs. control)*

CNDs Decrease the Expression of Pro-Inflammatory Genes Induced by oxLDL

OxLDL is another important mediator of macrophage activity in the development of atherosclerotic plaques. Therefore, I also investigated the impact of oxLDL induced expression of pro-inflammatory genes in THP-1 human monocyte-derived macrophages. Cells were treated with 25, 50, and 100 µg/mL oxLDL in HBSS for 6 hours. Using qRT-PCR, the relative gene expression of IL-8 was analyzed. As shown in Figure 8, oxLDL significantly increased ($P< 0.05$) IL-8 expression in cells treated with 50, and 100 µg/mL oxLDL. To better replicate physiological conditions, 100 µg/ml was the concentrations chosen for co-treatments. For the co-treatments, THP-1 human monocyte-derived

macrophages were treated with CND concentrations of 0.01, 0.1, and 0.3 mg/ml and 100 µg/ml oxLDL for 6 hours. Gene expression levels of IL-8, IL-1β, CCL2, and TNF-α were measured using q-RT-PCR. At all tested concentrations, cell cotreated with CNDs displayed decreased ($P < 0.05$) gene expression of IL-8 (Fig 9A), IL-1β (Fig 9B), CCL2 (Fig 9C), and TNF-α (Fig 9D) compared to cells treated with oxLDL alone.

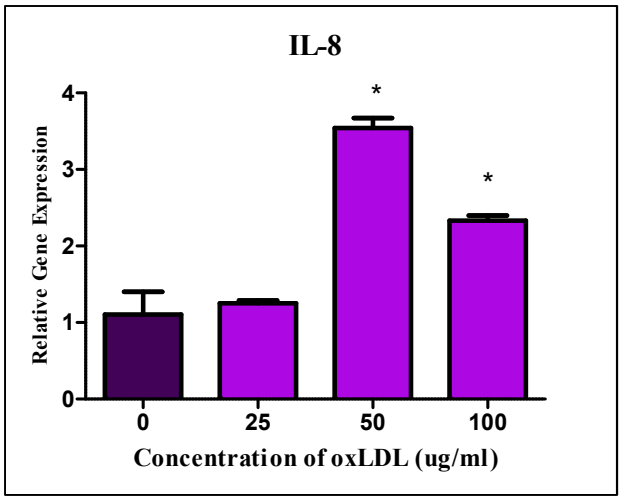

Figure 8. Dose-dependent Response due to OxLDL. THP-1 human monocyte-derived macrophages were treated with various concentrations of oxLDL for 6 hours in HBSS.A significant increase in IL-8 expression occurred when treated with 50, and 100 µg/ml oxLDL. GAPDH was the housekeeping gene. *All data represent mean ± SEM. (n = 3, P < 0.05 vs. control)*

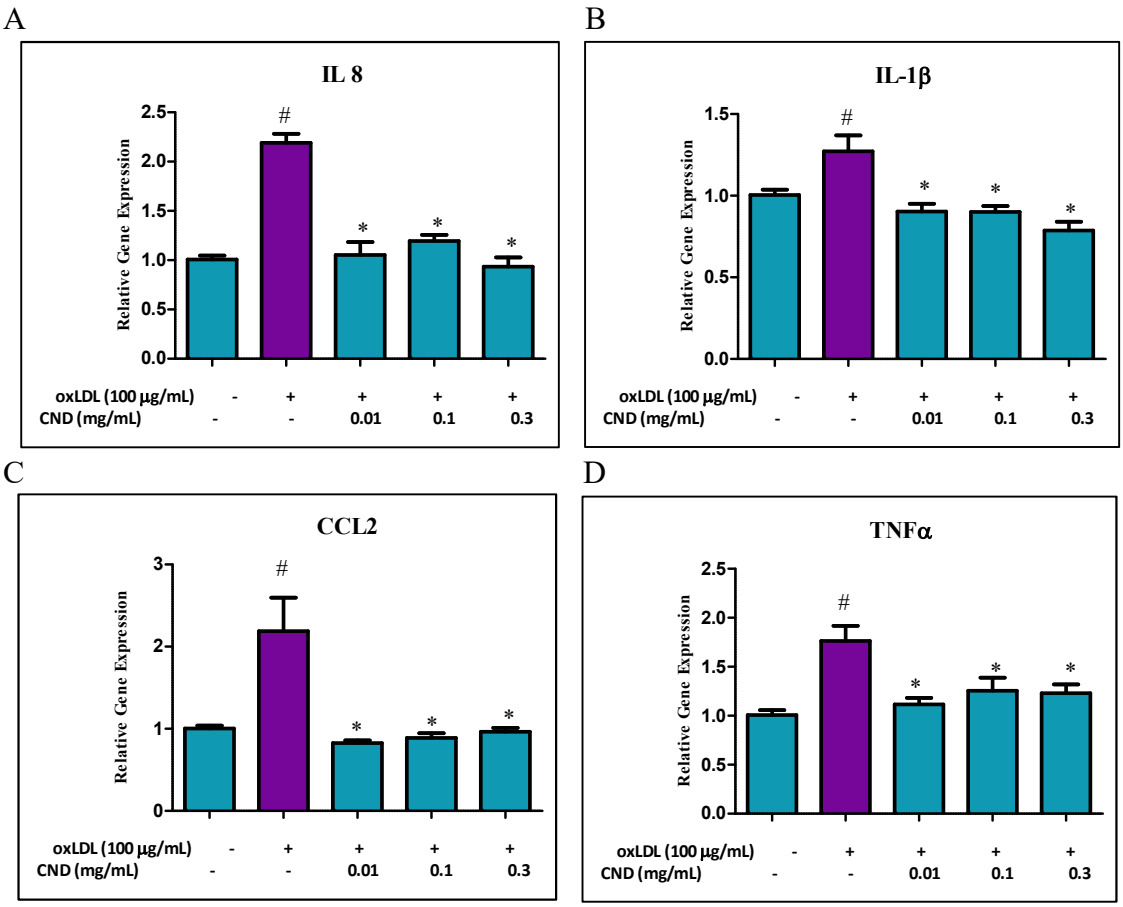

Figure 9. CNDs Decrease the Expression of Pro-Inflammatory Genes Induced by OxLDL in THP-1 Human Monocyte-Derived Macrophages. THP-1 human monocyte-derived macrophages were cotreated with 0.01-0.3 mg/mL CNDs and 100 µg/mL oLDL for 6 hours in HBSS. RNA was isolated, converted to cDNA, and asssayed for IL-8, IL -1β, CCL2, and TNF-α using SYBR green qRT-PCR reagents via QuantStudio 3. (a) Shows a significant decrease in IL-8 expression when cotreated 100 µg/mL oxLDL and 0.01-0.3 mg/mL CNDs of 6 hours in HBSS. (b) Shows a significant decrease in IL -1β expression when cotreated 100 µg/mL oxLDL and 0.01-0.3 mg/mL CNDs of 6 hours in HBSS. (c) Shows a significant decrease in CCL2 expression when cotreated with 100 µg/mL oxLDL and 0.01-0.3 mg/mL CNDs of 6 hours in HBSS. (d) Shows a significant decrease in TNF-α expression when cotreated with 100 µg/mL oxLDL and 0.01-0.3 mg/mL CNDs of 6 hours in HBSS. GAPDH was the housekeeping gene. All data represent mean ± SEM. (n = 9, #, $P < 0.05$ vs. control, * $P < 0.05$ vs. TNF-α)

Effect of CNDs on Lipid Uptake

When macrophages are exposed to oxLDL, they internalize the lipids and differentiate into foam cells, which accumulate within developing plaques. Oil Red O (ORO) staining was conducted to visualize and quantifiy lipid accumulation. THP-1 human monocyte-derived macrophages were treated 100 μg/mL oxLDL and 0.01-0.3 mg/mL CNDs of 6 hours. Cells were fixed, stained, and viewed using a Keyence BZ-X710 fluorescence microscope, using ORO staining technique. Figure 10 shows images of stained THP-1 human monocyte-derived macrophages. The lipid within cells that have accumulated oxLDL stained red, resulting in a significant number of dark red granules within cells treated with oxLDL alone compared to untreated cells, which contained few granules. CND cotreated macrophages displayed significantly less ORO staining. This staining was quantified by counting the ORO stained cells; cells with 30% or more of their area containing red granules were considered stained. THP-1 human monocyte-derived macrophages cotreated with CNDs displayed a significantly lower percentage ($P < 0.05$) of ORO stained cell compared to macrophages treated with oxLDL alone (Fig 11).

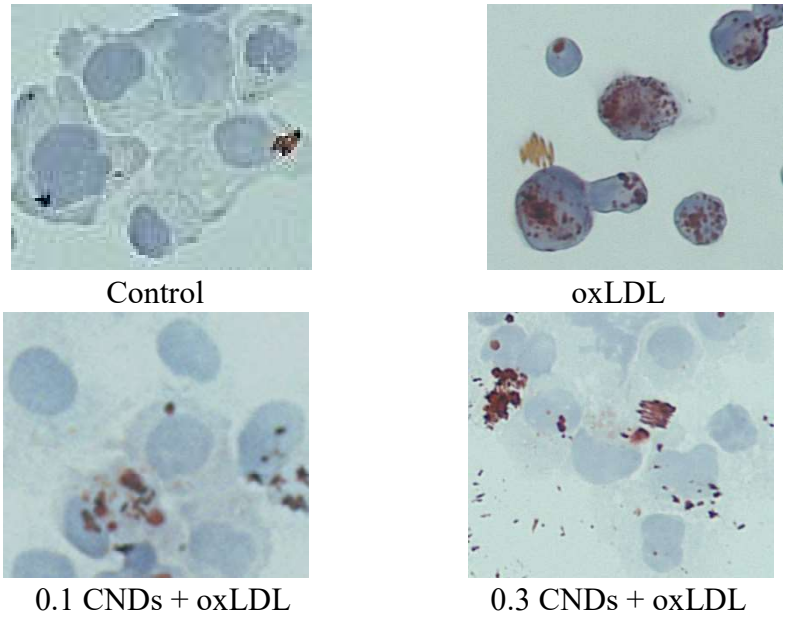

Figure 10. Representative Oil Red O Staining of Macrophages. THP-1 human monocyte-derived macrophages were co-treated with 100 µg/mL oxLDL and CNDs for 6 hours in HBSS. Cells were stained with ORO stain and observed and photographed using Keyence fluorescence microscope. Cells with dark red granules contains internalized oxLDL. From left to right, top row: control, 100 µg/mL oxLDL alone. bottom row: 0.1 mg/mL CNDs and 100 µg/mL oxLDL, 0.3 mg/mL CNDs and 100 µg/mL oxLDL. Magnification of images is x1000.

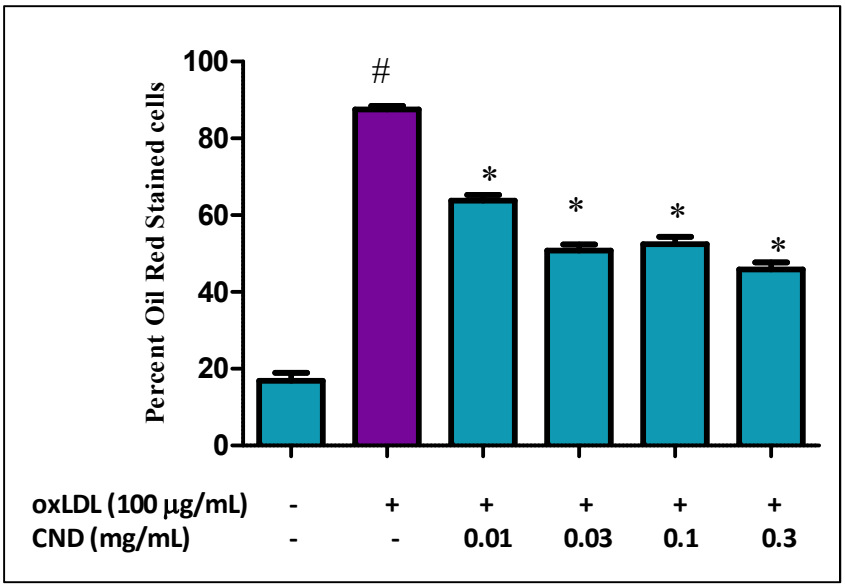

Figure 11. CNDs Reduce OxLDL Induced Lipid Uptake. THP-1 human monocyte-derived macrophages were co-treated with 100 µg/mL oxLDL and 0.01-0.3 mg/mL CNDs for 6 hours in HBSS. Cells were stained with ORO stain and observed and photographed using a Keyence fluorescence microscope. Cells whose area were 30% or more stained red were counted as stained. There was a significant decrease in the percentage of cells stained with ORO when cotreated with oxLDL and all concentrations of CNDs. All data represent mean ± SEM. (n = 6, #,$P < 0.05$ vs. control, * $P < 0.05$ vs. oxLDL)

CNDs Reduce TNF-α Mediated and OxLDL Mediated NF-κB Activity

NF-κB activation is associated with inflammatory diseases such as atherosclerosis and can be mediated by TNF-α or by oxLDL. Therefore, I examined the effect of CNDs on the NF-κB activation induced by TNF-α and oxLDL. NF-κB RAW264.7 cells were cotreated with 0.01-0.3 mg/mL CNDs and either 30 ng/mL TNF-α for 24 hours or 100 µg/mL oxLDL for 6 hours. After Coelenterazine was added as a substrate to *Renilla* luciferase, the luminescence intensity of the light produced was measured. TNF-α and oxLDL alone significantly increased ($P< 0.05$) NF-κB activity compared to untreated

cells (Fig 12). CNDs significantly reduced (P<0.05) NF-κB activity compared to TNF-α alone (Fig 12A) and oxLDL alone (Fig 12B).

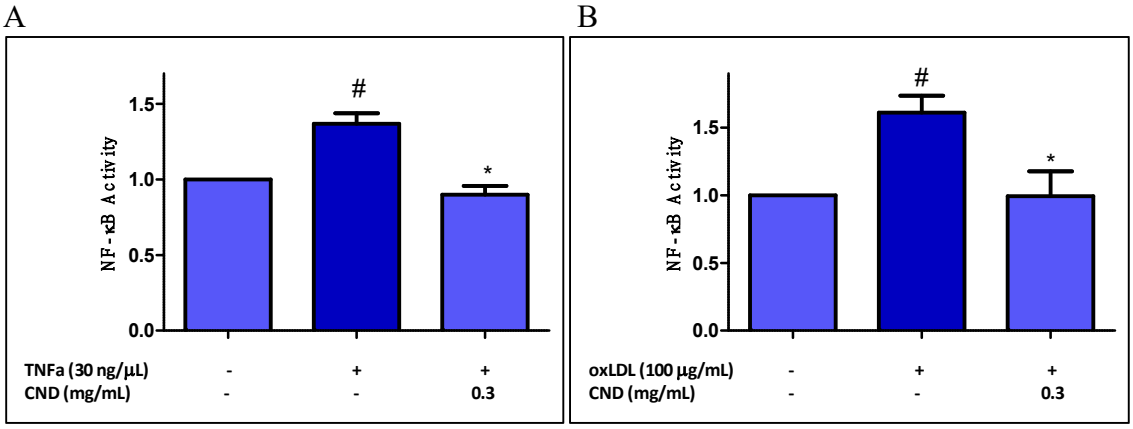

Figure 12. CNDs Reduce TNFα Mediated and OxLDL Mediated NF-κB Activity in NF-κB RAW264.7 Macrophages. (a) NF-κB RAW264.7 cells were cotreated with 0.3 mg/mL CNDs and 30 ng/mL TNF-α for 24 hours in HBSS. (b) NF-κB RAW264.7 cells were cotreated with 0.3 mg/mL CNDs and 100 µg/mL oxLDL for 6 hours in HBSS. 1 µM Coelenterazine was added as a substrate and luminescence was read directly after using Biotech Synergy 2 plate reader. All data represent mean ± SEM. (n = 3, #, P < 0.05 vs. control, * P < 0.05 vs. TNF-α)

CNDs Reduce OxLDL Induced Toxicity

At high concentrations, oxLDL can cause cytotoxicity through increased oxidative stress. Because of CNDs ability to scavenge free radicals and reduce oxidative stress, MTT assay, which assesses mitochondrial activity, was used to determine the effect of CNDs on THP-1 human monocyte-derived macrophages that were cotreated with cytotoxic concentrations of oxLDL. Cells were treated with 0 – 500 µg/mL oxLDL for 6 hours. Compared to untreated cells, cells treated with 400 and 500 µg/mL oxLDL displayed a significant decrease (P< 0.05) in cell viability (Fig 13A). THP-1 human

monocyte-derived macrophages were then cotreated with 400 µg/mL oxLDL and 0.1 and 0.3 mg/mL CNDs for 6 hours. Cells treated with both concentrations of CNDs displayed a significant increase ($P < 0.05$) in cell viability compared to cells treated with oxLDL alone (Fig 13B).

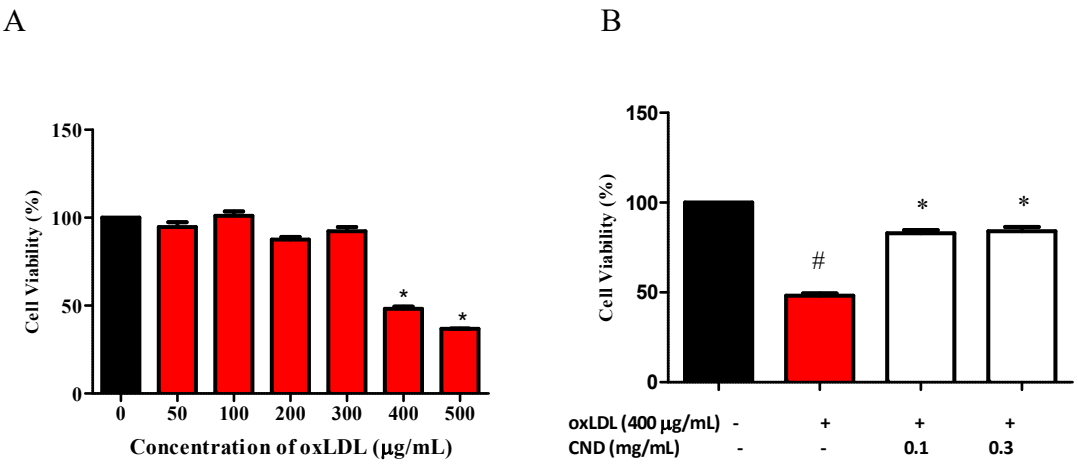

Figure 13. CNDs Reduce OxLDL Induced Toxicity. Cell viability was determined via MTT assay. (a) THP-1 human monocyte-derived macrophages were treated with 0 – 500 µg/mL oxLDL of 6 hours in HBSS. Compared to the control, the viability of cells treated with 400 and 500 µg/mL was significantly decreased. (b) THP-1 human monocyte-derived macrophages were co-treated with 400 µg/mL oxLDL and 0.1-0.3 mg/mL CNDs of 6 hours in HBSS. Cotreatment significantly increased cell viability compared to cells treated with oxLDL alone. All data represent mean ± SEM. (n = 3, #, $P < 0.05$ vs. control, * $P < 0.05$ vs. oxLDL)

CHAPTER IV

DISCUSSION

This study examines the impact of CNDs in the context of TNF-α and oxLDL mediated-inflammation. While displaying significant time- and dose- depedent intracellular uptake, CNDs do not significantly alter cell viability. CNDs significantlydecrease expression of proinflammatory mediators, ICAM and VCAM, and proinflammatory cytokines, IL-8, IL-1β, and CCL2 induced by TNF-α. CNDs also significantly decrease expression of proinflammatory cytokines, IL-8, IL-1β, CCL2, and TNF-α induced by oxLDL. CNDs significantly decrease lipid uptake in oxLDL cotreated cells, as indicated by Oil Red O staining, and decrease oxLDL induced cytotoxicity assessed via MTT. CNDs do not significantly alter gene expression of Phase II antioxidant enzymes, GCLc and NQO1. However CNDs do decrease NF-κB activity mediated by TNF-α and oxLDL.

Atherosclerosis is induced and mediated by inflammation, initiating with damage to endothelial cells, and recruitment of monocytes [7]. Macrophages derived from recruited monocytes propagate inflammation and eventual plaque formation by secreting inflammatory cytokines, like TNF-α, and ingesting cellular debris, including oxidized low-density lipoproteins (oxLDL) [8]. This lipid accumulation leads to foam cell differentiation, which adds to the progressing plaque and decreasing diameter of the blood vessel [6]. THP-1 human monocyte-derived macrophages were used as a model in

this study. This well-established cell line is widely used to study the function and regulation of monocytes and macrophages within the cardiovascular system [37]. THP-1 cells were induced to differentiate into macrophages by 12-O-tetradecanoylphorbol-13-acetate (TPA) treatment, which increases scavenger receptor CD36 expression and decreases LDL receptor expression [38]. Unlike the LDL receptor, expression of CD36 is upregulated in response to increased intracellular lipid concentration. Thus, this increase in scavenger receptor expression enhances internalization of oxLDL [39, 40]. Differentiated THP1 cells then can be become foams cells, allowing THP-1 cells to act as a model of monocyte-macrophage behavior during the progression of atherosclerosis [38]. These properties allowed THP-1 human monocyte-derived macrophages to be utilized to investigate the effects of CNDS on TNF-α and oxLDL induced inflammation.

Within atherosclerotic lesions, macrophages act as intermediaries by both responding to and exacerbating inflammation. Monocytes are recruited to the site of inflammation by pro-inflammatory cytokines, where they can differentiate into macrophages and begin secreting pro-inflammatory cytokines in response [6]. Pro-inflammatory mediators include VCAM and ICAM which facilitate leukocyte extravasation. IL-8 recruits and activates monocytes and neutrophils to the site of inflammation [41]. This cytokine also induces CXCR2-expressing monocytes to firmly adhere to endothelial cells [41]. CCL2 also facilitates the migration of neutrophils and targets antigen-presenting cells, T cells, and monocytes to undergo leukocyte extravasation [6]. IL-1β promotes leukocyte adhesion to ECs, smooth muscle cell proliferation, and production of inflammatory mediators in leukocytes [42]. In this study,

THP-1 human monocyte-derived macrophages displayed a dose-dependent increase in gene expression of the pro-inflammatory mediators, IL-8, VCAM, and ICAM when treated with 0-10 ng/mL TNF-α (Fig 5). CNDs, when cotreated with TNF-α, significantly decrease the expression of pro-inflammatory cytokines and mediators: ICAM, VCAM, IL-8, CCL2, and IL-1β (Fig 6). We demonstrated for the first time that CNDs reduce TNF-α induced inflammation in THP-1 human monocyte-derived macrophages.

In additional to TNF-α, oxLDL is another crucial mediator for macrophage activity in the development of atherosclerotic plaques [12]. When macrophages are activated, they increase the expression of scavenger receptors and toll-like receptors (TLR), which bind to and mediate the internalization of oxLDL [10]. This increases ROS formation during the oxidative burst, further oxidizing unaltered LDL, and increases secretion of proinflammatory cytokines, including IL-8, CCL2, IL-1β, and TNF-α [6, 12, 15]. THP-1 human monocyte-derived macrophages treated with 50 and 100 μg/mL oxLDL significantly increased gene expression of IL-8. Cotreatment with CNDs at concentrations as low as 0.01 mg/mL decreased expression of IL-8, CCL2, IL-1β, and TNF-α (Fig 9). Our results suggest that CNDs decrease oxLDL induced inflammation. The previous study of another nanoparticle, fullerene derivatives (FDs), displayed similar findings [43]. In U937 human monocyte-derived macrophages when treated with FDs, oxLDL induced secretion of TNF-α and cell-surface expression of ICAM-1 significantly decreased [43]. Gene expression levels of IL-8 and CCL2 also decreased in oxLDL and FD cotreated cells compared to cell treated with oxLDL alone [43]. While previous studies have examined the effect of other classes of nanoparticles on oxLDL mediated

inflammation in macrophages, this study for the first time, reports that CNDs reduce oxLDL induced inflammation in THP-1 human monocyte-derived macrophages.

After macrophages internalize oxLDL, they differentiate into foam cells, which accumulate within developing plaques**.** These foam cells continue secreting inflammatory cytokines, generating a positive feedback loop of monocyte recruit, differentiation, and lipid accumulation [15]. In this study, THP-1 human monocyte-derived macrophages cotreated with oxLDL and CNDs displayed significantly less ORO staining compared to cells treated with LDL alone (Fig 11). This finding is consistent with previous research, which found that fullerene derivatives significantly decreased lipoprotein-induce lipid accumulation within monocyte-derived macrophages [43]. In this study, we report that anti-inflammatory CNDs significantly reduce the internalization of oxLDL within THP-1 human monocyte-derived macrophages and thus affect lipid metabolism (Fig 11). It remains unknown if this trend also exists *in vivo*. Future research should include examining the effect of CNDs on lipid accumulations within the blood vessel of an animal model for atherosclerosis.

We further examined the possible cellular mechanisms influencing the anti-inflammatory effects of CNDs against TNF-α and oxLDL in macrophages. It was hypothesized that CNDs are taken up by the cells to exhibit their effects in THP-1 human monocyte-derived macrophages. The emission peak of the tested CNDs was about 460 nm (Fig. 3A). This photoluminescence allowed us to examine the intracellular uptake of CNDs by THP-1 human monocyte-derived macrophages using spectrofluorometry. Dose-dependent and time-dependent CNDs uptake was observed (Fig 4). While this data

supports the idea that CNDs were intracellularly taken up by THP-1 human monocyte-derived macrophages, the pathways by which CNDs enter the cells remains unknown.

Reactive oxygen species are known to induce inflammation by causing oxidative stress; increased oxidative stress can regulate the synthesis of pro-inflammatory cytokines and antioxidant molecules and enzymes [15, 44, 45]. These enzymes include glutathione reductase (GR), glutathione peroxidase (GPx), glutathione S-transferase (GST), NAD(P)H: quinone oxidoreductase 1 (NQO1), superoxide dismutase (SOD) and catalase [15, 46]. These antioxidant molecules and enzymes then reduce oxidative stress and resulting inflammation by neutralizing ROS. Previous studies have found that CNDs possess antioxidant properties by directly scavenging free radicals [32-34, 47]. This suggests that direct scavenging for radicals and thus decreasing oxidative stress may be the method by which CNDs reduce inflammation induced by TNF-α and oxLDL.

In this study, we further investigated whether CNDs also induce endogenous antioxidants and phase 2 enzymes in macrophages, which inhibit ROS and reduce oxidative and inflammatory responses, as mentioned above. GCLc is one of two subunits of Gamma-glutamate cystine ligase (GCL), an enzyme involved in the synthesis of glutathione (GSH) [48]. NAD(P)H: quinone oxidoreductase 1 (NQO1) detoxifies xenobiotic by reducing quinones to hydroquioine [46]. This study found that when THP-1 human monocyte-derived macrophages were treated with 0.01 to 0.3 mg/mL CNDs for 24 hours, the gene expression level of GCLc and NQO1 did not differ significantly from untreated cells. These results indicate that the antinflammatory activity of CNDs is not mediated through upregulation of an antioxidant mechanism. However, only one-time

point was tested with a limited number of concentrations of CNDs and only two target genes. Future studies can measure the gene expression of other antioxidant enzymes like GR, GPx, GST, SOD, and catalase. The activity of GSH and NQO1, as well as other antioxidant enzymes, can also be assessed.

We next investigated the cytoprotective effects of CNDs on oxLDL induced toxicity in macrophages, to further verify the antioxidant properties of CNDs. OxLDL, unlike unmodified LDL, is partly resistant to lysosomal degradation and therefore accumulate within lysosomes [49]. This leads to lysosomal rupture and the release of lipid peroxides, toxic aldehydes, and ROS [49]. As concentrations of oxLDL increases, this free radical production increase and leads to damage to cellular macromolecules [15]. The effect of CNDs on oxLDL induced cytotoxicity was assessed via MTT assay. THP-1 human monocyte-derived macrophages were incubated with 0 to 500 μg/mL oxLDL for 6 hours and displayed a significant decrease in cell viability at 400 and 500 μg/mL oxLDL compared to untreated cells (Fig 13A). However, cotreatment with 0.1 to 0.3 mg/mL CNDs increased cell viability from 50% in oxLDL treated cells to 80% in CNDs cotreated cells (Fig 13B). This significant increase in cell viability indicates that CNDs protect against oxLDL-induced cell death and suggests the mechanism is due to CNDs ability to scavenge free radicals and subsequently reduce oxidative stress.

Previous studies show that oxLDL can elicit either necrosis or apoptosis by activating calcium-dependent endonucleases involved in apoptotic chromatin cleavage and calcium-dependent protease involved in necrotic cytoskeletal alterations [50, 51]. OxLDL can also trigger the release of cytochrome c into the cytosol via the

mitochondrial apoptosis pathway, leading to activation of initiator caspase-9 and executioner caspases-3/6/7 [52, 53]. Necrotic and apoptotic macrophages contribute to progressing plaques by remaining at the site of inflammation and forming a necrotic core [11]. Since both apoptotic and necrotic cell death are observed in oxLDL exposed macrophages, future studies should examine the impact of CNDs on different models of cell death. Future studies should also determine how CNDs modulate the ratio of pro-inflammatory M1 macrophages to anti-inflammatory M2 macrophages; this is especially notable because M2 macrophages are more susceptible to oxLDL cytotoxicity compared to M1 macrophages and monocytes so a change in the M1:M2 ratio could alter the ratio of viable, apoptotic, and necrotic cells [54].

Atherosclerosis is correlated with nuclear factor Kappa B (NF-κB) activation. This pathway can be activated by proinflammatory cytokines, particularly TNF-α and IL-1, or by the binding of ligands like oxLDL to Toll-like receptors (TLRs) [55]. Activation of the NF-κB pathway leads to increased secretion of proinflammatory cytokines and chemokines in macrophages. In this study, the effect of CNDs on TNF-α- and oxLDL-induced NF-κB activation was assessed. A significant increase in relative NF-κB activity was observed in NF-κB RAW264.7 cells treated with TNF-α alone (Fig12A), and oxLDL alone (Fig 12B) compared to untreated cells (Fig 12). This indicates that NF-κB activation is associated with the inflammatory response induced by TNF-α and oxLDL. When RAW264.7 cells were cotreated with 0.3 mg/mL and 30 ng/μL TNF-α or 100 μg/mL oxLDL, there was a significant decrease in relative NF-κB activity (Fig 12). This suggests that CNDs decrease both TNF-α and oxLDL induced inflammation by

modulating the NF-κB signaling pathway. This finding is also consistent with Plotkin's research of fullerene derivatives. The research found that their nanoparticles reduced oxLDL induced inflammation by reducing NF-κB protein expression and modulating the NF-κB pathway [43]. After NF-κB activation, Inhibitor of κB (IκBα) dissociated from the p65/ p50 subunits of NF-κB; the p65 or p50 subunits then translocate to the nucleus and bind to the promotor of inflammatory genes and induce transcription [56, 57]. To verify the effect of CNDs on NF-κB activation, future research could assess NF-κB nuclear translocation by measuring subunits p65/ p50 and IkBα protein level in the nucleus and in the cytoplasm of THP-1 human monocyte-derived macrophages via Western Blotting.

In summary, this study examined the impact of CNDs on TNF-α and oxLDL induced inflammation in THP-1 human monocyte-derived macrophages. It was demonstrated that CNDs do not cause cytotoxicity in macrophages and display dose-dependent and time-dependent intracellular uptake. CNDs significantly decrease TNF-α induced gene expression of IL-8, ICAM, VCAM, CCL2, and IL-1β, vital molecules in the recruitment and differentiation of monocytes to the site of inflammation during atherosclerosis. CNDs cotreatment also significantly reduced IL-8, CCL2, IL-1β, and TNF-α expression in the context of oxLDL induced inflammation. Oil Red O Staining also demonstrated that CNDs decrease oxLDL induced lipid accumulation, suggesting that CNDs reduce foam cell formation. When the effects of CNDs on oxLDL induced cytotoxicity was assessed via MTT, CNDs significantly increased cell viability, ameliorating the cytotoxicity. While CNDs did not alter gene expression of phase II

enzymes, GCLc and NQO1, future studies should further examine the impact of CNDs on other antioxidants and antioxidant enzymes. Additionally, CNDs ameliorated both TNF-α and oxLDL induced NF-κB activity, and thus moderate NF-κB modulated inflammation. Collectively, this research provides evidence for the ability of CNDs to modulate TNF-α and oxLDL induced inflammation and resulting atherosclerosis.

REFERENCES

1. Benjamin, E.J., *Heart Disease and Stroke Statistics'2017 Update: A Report from the American Heart Association.* Circulation, 2017. **135**(10): p. 146.

2. National Center for Chronic Disease Prevention and Health Promotion, D.f.H.D.a.S.P. *Heart Disease Fact Sheet*. 2017; Available from: https://www.cdc.gov/dhdsp/data_statistics/fact_sheets/fs_heart_disease.htm.

3. WHO. *Cardiovascular disease*. 2018 [cited 2018; Available from: http://www.who.int/cardiovascular_diseases/en/.

4. Hruby, A. and F.B. Hu, *The Epidemiology of Obesity: A Big Picture.* PharmacoEconomics, 2015. **33**(7): p. 673-689.

5. Yazdanyar, A. and A.B. Newman, *The burden of cardiovascular disease in the elderly: morbidity, mortality, and costs.* Clinics in geriatric medicine, 2009. **25**(4): p. 563-vii.

6. Bobryshev, Y.V., et al., *Macrophages and Their Role in Atherosclerosis: Pathophysiology and Transcriptome Analysis*. Vol. 2016. 2016. 13.

7. Hansson, G.K., *Mechanisms of disease: Inflammation, atherosclerosis, and coronary artery disease.* New England Journal of Medicine, 2005. **352**(16): p. 1685-1695.

8. Fenyo, I.M. and A.V. Gafencu, *The involvement of the monocytes/macrophages in chronic inflammation associated with atherosclerosis.* Immunobiology, 2013. **218**(11): p. 1376-1384.

9. Libby, P., *Inflammation in atherosclerosis.* Arteriosclerosis, Thrombosis, and Vascular Biology, 2012. **32**(9): p. 2045-2051.

10. Galdiero, M.R., S.K. Biswas, and A. Mantovani, *Polarized Activation of Macrophages*, in *Macrophages: Biology and Role in the Pathology of Diseases*, S.K. Biswas and A. Mantovani, Editors. 2014, Springer New York: New York, NY. p. 37-57.

11. Fredman, G. and I. Tabas, *Macrophages Govern the Progression and Termination of Inflammation in Atherosclerosis and Metabolic Diseases*, in *Macrophages:*

Biology and Role in the Pathology of Diseases, S.K. Biswas and A. Mantovani, Editors. 2014, Springer New York: New York, NY. p. 387-403.

12. Alique, M., et al., *LDL biochemical modifications: a link between atherosclerosis and aging.* Food & nutrition research, 2015. **59**: p. 29240-29240.

13. Janabi, M., et al., *Oxidized LDL-induced NF-kappa B activation and subsequent expression of proinflammatory genes are defective in monocyte-derived macrophages from CD36-deficient patients.* Arterioscler Thromb Vasc Biol, 2000. **20**(8): p. 1953-60.

14. Howell, K.W., et al., *Toll-like receptor 4 mediates oxidized LDL-induced macrophage differentiation to foam cells.* J Surg Res, 2011. **171**(1): p. e27-31.

15. Peluso, I., *Oxidative stress in atherosclerosis development: The central role of LDL and oxidative burst.* Endocrine, Metabolic and Immune Disorders-Drug Targets, 2012. **12**(4): p. 351-360.

16. Libby, P., *Inflammation in atherosclerosis.* Nature, 2002. **420**: p. 868.

17. Zalba, G., *Vascular oxidant stress: Molecular mechanisms and pathophysiological implications.* Journal of Physiology and Biochemistry, 2000. **56**(1): p. 57-64.

18. Castaneda, O.A., et al., *Macrophages in oxidative stress and models to evaluate the antioxidant function of dietary natural compounds.* Journal of Food and Drug Analysis, 2017. **25**(1): p. 111-118.

19. Beltowski, J., *Statins and modulation of oxidative stress.* Toxicology Mechanisms Methods, 2005. **15**(2): p. 61-92.

20. Hagedorn, J., *Association of statins and diabetes mellitus.* American Journal of Therapeutics, 2010. **17**(2): p. 52.

21. Jeppesen, U., *Statins and peripheral neuropathy.* European Journal of Clinical Pharmacology, 1999. **54**(11): p. 835-838.

22. Mammen, A.L. and A.A. Amato, *Statin myopathy: a review of recent progress.* Curr Opin Rheumatol, 2010. **22**(6): p. 644-50.

23. Hanif, K., *Reinventing the ACE inhibitors: Some old and new implications of ACE inhibition.* Hypertension Research, 2010. **33**(1): p. 11-21.

24. Hennekens, C.H. and W.R. Schneider, *The need for wider and appropriate utilization of aspirin and statins in the treatment and prevention of cardiovascular disease.* Expert Review of Cardiovascular Therapy, 2008. **6**(1): p. 95-107.

25. Perry, J.L., C.R. Martin, and J.D. Stewart, *Drug-delivery strategies by using template-synthesized nanotubes.* Chemistry, 2011. **17**(23): p. 6296-302.

26. Weissleder, R., *Imaging macrophages with nanoparticles.* Nature Materials, 2014. **13**(2): p. 125-138.

27. Briley-Saebo, K.C., et al., *Targeted iron oxide particles for in vivo magnetic resonance detection of atherosclerotic lesions with antibodies directed to oxidation-specific epitopes.* Journal of the American College of Cardiology, 2011. **57**(3): p. 337-347.

28. Ding, C., A. Zhu, and Y. Tian, *Functional Surface Engineering of C-Dots for Fluorescent Biosensing and in Vivo Bioimaging.* Accounts of Chemical Research, 2014. **47**(1): p. 20-30.

29. Sun, H., et al., *Graphene Quantum Dots-Band-Aids Used for Wound Disinfection.* ACS Nano, 2014. **8**(6): p. 6202-6210.

30. Miao, P., et al., *Recent advances in carbon nanodots: synthesis, properties and biomedical applications.* Nanoscale, 2015. **7**(5): p. 1586-1595.

31. Hoshino, A., et al., *Use of fluorescent quantum dot bioconjugates for cellular imaging of immune cells, cell organelle labeling, and nanomedicine: surface modification regulates biological function, including cytotoxicity.* Journal of Artificial Organs, 2007. **10**(3): p. 149-157.

32. Zhang, W., et al., *Antioxidant Capacity of Nitrogen and Sulfur Codoped Carbon Nanodots.* ACS Applied Nano Materials, 2018. **1**(6): p. 2699-2708.

33. Das, B., et al., *Carbon nanodots from date molasses: new nanolights for the in vitro scavenging of reactive oxygen species.* Journal of Materials Chemistry B, 2014. **2**(39): p. 6839-6847.

34. Zhang, W., Z. Zeng, and J. Wei, *Electrochemical Study of DPPH Radical Scavenging for Evaluating the Antioxidant Capacity of Carbon Nanodots.* The Journal of Physical Chemistry C, 2017. **121**(34): p. 18635-18642.

35. Kato, K., et al., *Studies on scavengers of active oxygen species. 1. Synthesis and biological activity of 2-O-alkylascorbic acids.* Journal of Medicinal Chemistry, 1988. **31**(4): p. 793-798.

36. Daugherty, A. *STAINING FROZEN TISSUE WITH OIL RED-O*. 2014; Available from: http://cvrc.med.uky.edu/sites/default/files/Oil-Red-O%20Staining.pdf.

37. Qin, Z., *The use of THP-1 cells as a model for mimicking the function and regulation of monocytes and macrophages in the vasculature.* Atherosclerosis, 2012. **221**(1): p. 2-11.

38. Johnson, A.C.M., et al., *Experimental Glomerulopathy Alters Renal Cortical Cholesterol, SR-B1, ABCA1, and HMG CoA Reductase Expression.* The American Journal of Pathology, 2003. **162**(1): p. 283-291.

39. Blanco, A. and G. Blanco, *Chapter 15 - Lipid Metabolism*, in *Medical Biochemistry*, A. Blanco and G. Blanco, Editors. 2017, Academic Press. p. 325-365.

40. Nicholson, A.C., et al., *CD36 in atherosclerosis. The role of a class B macrophage scavenger receptor.* Ann N Y Acad Sci, 2000. **902**: p. 128-31; discussion 131-3.

41. Apostolakis, S., et al., *Interleukin 8 and cardiovascular disease.* Cardiovasc Res, 2009. **84**(3): p. 353-60.

42. Libby, P., *Interleukin-1 Beta as a Target for Atherosclerosis Therapy: Biological Basis of CANTOS and Beyond.* J Am Coll Cardiol, 2017. **70**(18): p. 2278-2289.

43. Plotkin, J.D., et al., *NF-κB inhibitors that prevent foam cell formation and atherosclerotic plaque accumulation.* Nanomedicine: Nanotechnology, Biology and Medicine, 2017. **13**(6): p. 2037-2048.

44. Mittal, M., et al., *Reactive oxygen species in inflammation and tissue injury.* Antioxid Redox Signal, 2014. **20**(7): p. 1126-67.

45. Schieber, M. and N.S. Chandel, *ROS function in redox signaling and oxidative stress.* Current biology : CB, 2014. **24**(10): p. R453-R462.

46. Dinkova-Kostova, A.T. and P. Talalay, *NAD(P)H:quinone acceptor oxidoreductase 1 (NQO1), a multifunctional antioxidant enzyme and exceptionally versatile cytoprotector.* Arch Biochem Biophys, 2010. **501**(1): p. 116-23.

47. Ji, Z., et al., *Tuning the Functional Groups on Carbon Nanodots and Antioxidant Studies.* Molecules (Basel, Switzerland), 2019. **24**(1): p. 152.

48. Lu, S.C., *Glutathione synthesis.* Biochimica et biophysica acta, 2013. **1830**(5): p. 3143-3153.

49. Li, W., X.M. Yuan, and U.T. Brunk, *OxLDL-induced macrophage cytotoxicity is mediated by lysosomal rupture and modified by intralysosomal redox-active iron.* Free Radical Research, 1998. **29**(5): p. 389-398.

50. Escargueil-Blanc, I., R. Salvayre, and A. Nègre-Salvayre, *Necrosis and apoptosis induced by oxidized low density lipoproteins occur through two calcium-dependent pathways in lymphoblastoid cells.* FASEB Journal, 1994. **8**(13): p. 1075-1080.

51. Meilhac, O., et al., *Bcl-2 alters the balance between apoptosis and necrosis, but does not prevent cell death induced by oxidized low density lipoproteins.* FASEB Journal, 1999. **13**(3): p. 485-494.

52. Wintergerst, E.S., et al., *Apoptosis induced by oxidized low density lipoprotein in human monocyte-derived macrophages involves CD36 and activation of caspase-3.* Eur J Biochem, 2000. **267**(19): p. 6050-9.

53. Salvayre, R., et al., *Oxidized low-density lipoprotein-induced apoptosis.* Biochimica et Biophysica Acta (BBA) - Molecular and Cell Biology of Lipids, 2002. **1585**(2): p. 213-221.

54. Isa, S.A., et al., *M2 macrophages exhibit higher sensitivity to oxLDL-induced lipotoxicity than other monocyte/macrophage subtypes.* Lipids in Health and Disease, 2011. **10**(1): p. 229.

55. Lawrence, T., *The nuclear factor NF-kappaB pathway in inflammation.* Cold Spring Harbor perspectives in biology, 2009. **1**(6): p. a001651-a001651.

56. Hayden, M.S. and S. Ghosh, *Regulation of NF-κB by TNF family cytokines.* Seminars in immunology, 2014. **26**(3): p. 253-266.

57. Napetschnig, J. and H. Wu, *Molecular Basis of NF-κB Signaling.* Annual Review of Biophysics, 2013. **42**(1): p. 443-468.